Growth Analysis and Fracture Mechanics Based on Measured Stress Change near a Full-Size Hydraulic Fracture

Ken W Mills
SCT Operations Pty Ltd, Wollongong, Australia

Rob Jeffrey and Xi Zhang
CSIRO Petroleum, Melbourne, Australia

ABSTRACT This paper describes the successful measurement of stress changes induced in a crystalline rock mass adjacent to a full size hydraulic fracture. A hydraulic fracture was initially formed using water and subsequently reopened using cross linked gel. The stress changes measured during these treatments are compared with the results of 2-D numerical models. The full three dimensional stress changes were measured using four ANZI stresscells installed and tested in situ prior to the start of hydraulic fracturing. The instruments were installed in pairs in two boreholes located some 7-8m laterally and 17-20m above the injection point. The in situ stressfield at the site was such that the hydraulic fracture passed within approximately 5m of the instruments allowing the stress changes associated with the passage of the fracture tip to be monitored as well as the stresses induced in the rock by the hydraulic fracture once the fracture tip was well past. The instruments were logged at 15 second intervals throughout the hydraulic fracture treatments to provide a time history of the complete three dimensional stress changes that occurred as each hydraulic fracture grew toward and then passed close to the instruments.

The monitoring was undertaken as part of a larger project aimed at preconditioning a rock mass with multiple hydraulic fractures. The results of only two of the fractures are considered in this paper. Analysis of the other fractures is ongoing.

Analysis of the stress change data provides information about the fracture rate and mode of growth, orientation, and about the excess pressure acting inside the fracture to open it.

1. INTRODUCTION

Hydraulic fracturing has long been used to induce fractures in rock masses for reservoir stimulation and other purposes. However, it is rare to have the opportunity to measure the actual stress changes that are caused by a full scale hydraulic fracture as it grows. Recently, a study aimed at assessing the potential for using multiple hydraulic fractures to pre-condition a rock mass to increase caveability and reduce fragment size provided just such an opportunity.

The details of the site and the overall study results remain confidential as a condition of using the data, but the results of the stress change monitoring are of interest from a scientific perspective unrelated to the outcomes of the caveability study.

This paper describes the results of three dimensional stress change monitoring about two full size hydraulic fractures induced in a crystalline rock mass. An initial hydraulic fracture was made using water as the injection fluid. This fracture was later reopened using cross-linked gel.

2. STRESS CHANGE MONITORING

The stress change in the rock near the hydraulic fractures was measured using ANZI cells. These instruments are described in detail in Mills [1].

The ANZI cell is a soft, inflatable stress measurement instrument that measures the strain changes on the wall of a borehole induced by stress changes in the rock mass. In each instrument, eighteen electrical resistance strain gauges of various orientations are pressure bonded directly onto the borehole wall.

A multiple linear regression analysis of the strain changes measured by the instrument allows the complete three dimensional stress changes to be calculated. A high level of redundancy (only six of the eighteen strain readings are required to determine the full stress change tensor) provides a strong measure of the confidence that can be placed in the integrity of the result.

The stress change cells were installed in two BQ-size boreholes located north and south of the main fracture injection hole. The holes were drilled downward some 45m at 60° from horizontal. Two

ANZI cells were installed near the bottom of each hole. The instruments are hollow so two or more instruments can be installed in the same hole with the cable from the lower instrument passing up through the centre of the other instrument. Although all four instruments were successfully installed and tested, the signal from one of them was very noisy and has been ignored.

Table 1 gives the relative positions of the instruments and the injection point in a local coordinate system.

Table 1: Coordinates of Injection Point and Stress Change Instruments in Local Coordinate System

	Easting (m)	Northing (m)	Reduced Level (m)
Injection Point	838.08	765.66	550.5
AN1	826.60	772.46	567.77
AN2	827.87	772.56	565.62
AN3	829.65	757.28	565.19

In each treatment, the hydraulic fractures passed below the lower end of the 45m long holes so that the stress monitoring holes had no influence on the growth of the hydraulic fractures.

All the strain gauges on all the instruments were data logged at 15 second intervals throughout each of the hydraulic fracture treatments. The data logger was started well before each treatment commenced to provide a measure of the stability of the instruments prior to the onset of stress change.

On each instrument, a reference gauge isolated from any strain change was used to reduce some of the signal noise associated with the long cables. Any changes measured on the reference gauge are assumed to be signal noise that can be subtracted from the readings on other gauges. Using this approach, the signal noise was reduced to ±3μS. A triangular moving average function was applied to the data to reduce signal noise to about ±1μS.

3. STRESS MONITORING RESULTS

Fig. 1 shows an example of the strain changes measured on AN2 during the gel fracture. There are a number of characteristics about the results that give confidence in their integrity.

A strong agreement between independent strain gauges measuring strains on opposite sides of the borehole can be seen in Fig. 1. This correlation boosts confidence in the result as the strains on opposite sides of the borehole are equal in a material that is homogeneous, elastic and isotropic.

The clear correlation between opposite gauges is even more encouraging given the very low strain magnitudes involved.

A second characteristic of the strain changes that builds confidence in the results is the clear correlation between the measured strains and the timing of the hydraulic fracture treatment. The onset of strain changes coincides with the timing of the start of the injection. The strains start to drop away soon after injection stops and there is a further step changes when the packers are deflated and flow back occurs.

From an analytical perspective, the most compelling confirmation of the veracity of the results is the excellent correlation obtained from the strain analysis itself. Correlation coefficients of better than 0.99 on 12 degrees of freedom are consistently obtained from the multiple linear regression analysis of the eighteen independent strain readings. This correlation indicates a high level of confidence can be placed in the calculated stress changes and the measurement error is insignificant for most practical purposes.

The excellent correlation between the measurements obtained from independent instruments adds further to the conclusion that the overall integrity of the results is high and the measurements are convincing point measurements of stress change in the vicinity of the hydraulic fracture. All three stress change monitoring instruments show essentially similar behaviour.

Intersections of the hydraulic fractures in other monitoring boreholes indicate that hydraulic fractures at this site develop in an orientation that is near vertical and striking at about 10°GN.

For near vertical hydraulic fractures, the plan view presentation is the easiest to visualize. Fig. 2 shows the measured stress change history plotted as vectors in plan view during the initial water fracture. Fig. 3 shows the measured stress change history when the same fracture was re-opened using cross linked gel.

The major stress change component develops approximately normal to the fracture plane with a magnitude of 0.5-0.8MPa. The other two stress change components that act in the plane of the hydraulic fracture are less than 10-20% of the magnitude reached by the major stress change.

The pattern of stress changes measured is essentially similar for all the instruments and all the treatments. The stages identified are:

1. A steady state prior to the commencement of the treatment.
2. A tensile going stress change that starts almost simultaneously with breakdown.
3. A compressive going stress change that starts a short time later (within 1.5 minutes) and continues to increase throughout the treatment.

The major horizontal stress change indicated by the measurements is oriented at between 265°GN and 280°GN. This orientation is consistent with a vertical hydraulic fracture with a north-south alignment.

Differences between the water treatment and the gel treatment include:

1. The magnitude of the tensile going stress change is less in the gel treatment.
2. The final magnitude of the compression going stress change is greater in the gel treatment.

The magnitude of the compressive stress change measured during the water fracture treatment reaches up to 0.5MPa. The magnitude of the compressive stress changes measured during the gel treatment is higher at 0.8MPa.

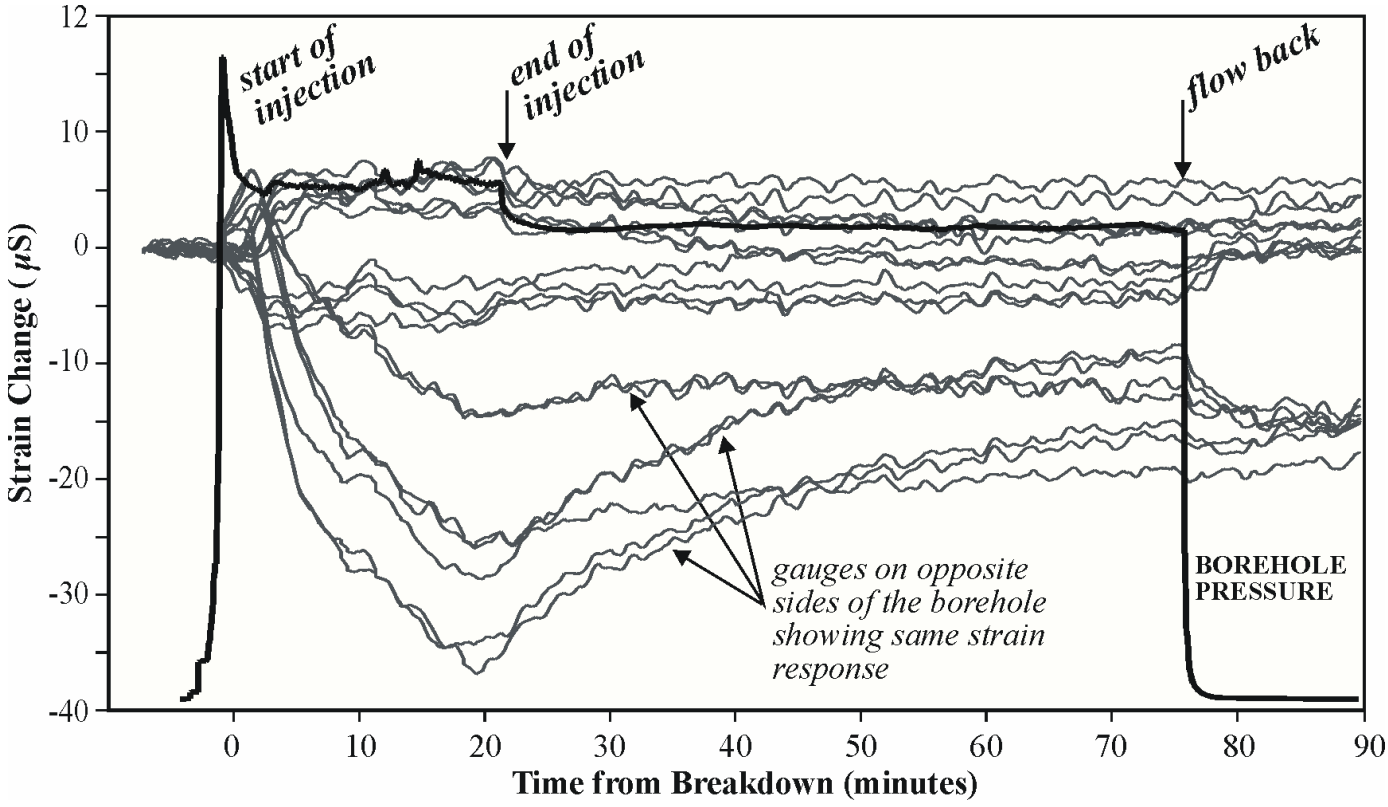

Fig. 1: Strain change measured by cell AN2 during fracture treatment 1. The pressure record from fracture 1 is superimposed on the strain data.

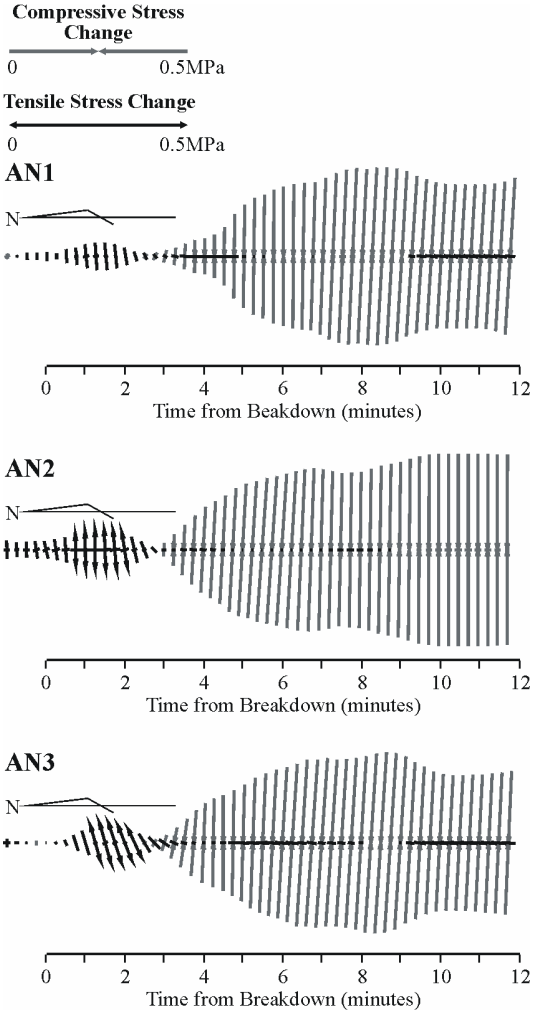

Fig. 2: Stress change recorded by three cells during the first 12 minutes of fracture treatment 1 (water frac).

4. STRESS INDUCED BY A FRACTURE

The stress change produce by an opening or shear fracture in an isotropic elastic material can be calculated for some cases using analytical solutions. More complicated fracture geometry and loading can be considered by using numerical models.

A plane strain and axisymmetric or radial fracture geometries are used below as models to obtain stress change around an idealized fracture. The stress and displacement fields around fractures with these geometries have been solved for analytically and results form those solutions are used here to obtain a stress field for comparison to the measured stress change data. The fracture is oriented along a coordinate axis in both the plane strain and radial case (Fig. 4).

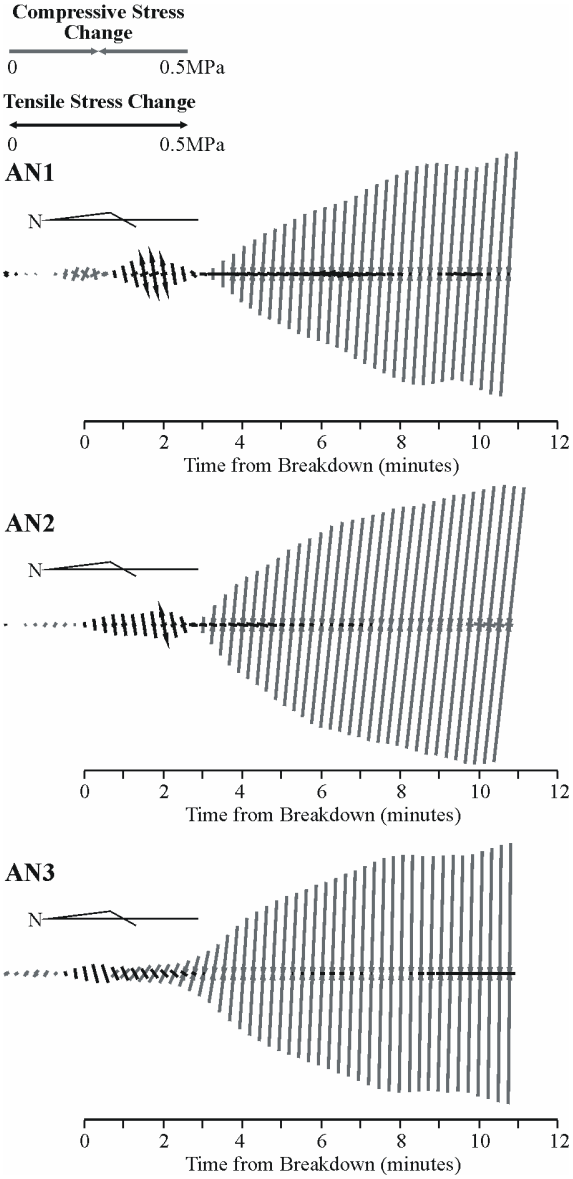

Fig. 3: Stress change recorded by the three cells during fracture treatment 2 (gel frac).

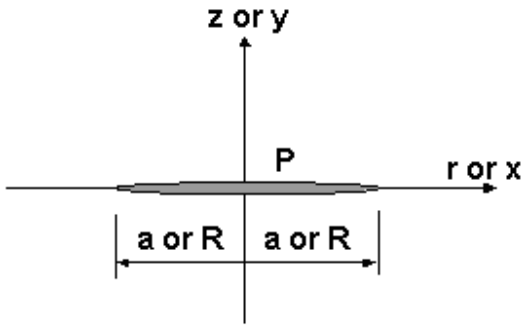

Fig. 4: Fracture coordinate and geometry. The x-y coordinate system applies to the plane strain fracture and the r-z system applies to the radial fracture.

4.1. Plane strain fracture - uniform pressure

The plane strain fracture is of length 2a and lies along the x axis (Fig. 4). It is pressurized by a uniform pressure P. Simple expressions for the stresses exist for lines extending along the coordinate axes.

The stresses σ_x and σ_y along the line extending from the fracture tip in the direction of x, induced by the internal pressure, P, are given by (Pollard and Segall [2]):

$$\sigma_y = P\left[\frac{x}{\left(x^2 - a^2\right)^{1/2}} - 1\right] \qquad (1a)$$

$$\sigma_x = P\left[\frac{x}{\left(x^2 - a^2\right)^{1/2}} - 1\right] \qquad (1b)$$

$$\sigma_{xy} = 0 \qquad (1c)$$

For internal pressure loading, σ_x and σ_y are both tensile and have the same magnitude along the x-axis.

These stress components along the y-axis are given by:

$$\sigma_y = P\left[\frac{y^3}{\left(y^2 + a^2\right)^{3/2}} - 1\right] \qquad (2a)$$

$$\sigma_x = P\left[\frac{\left(y^3 + 2ya^2\right)}{\left(y^2 + a^2\right)^{3/2}} - 1\right] \qquad (2b)$$

$$\sigma_{xy} = 0 \qquad (2c)$$

Along the y-axis σ_x and σ_y are both compressive near the fracture plane but σ_x becomes slightly tensile at distances greater than about 0.9a from the fracture.

4.2. Radial fracture – uniform pressure

The stress and displacement distribution around an axisymmetric or radial fracture is given by Sneddon [3]. The solution equations for stress have been coded into a program and evaluated along lines extending from the center of the fracture outward at angles of 0, 30, 45, and 90 degrees. Fig. 5 contains the results of this calculation.

The (r,z) coordinate system is used and the radius of the axisymmetric fracture is R. The measured stress change magnitudes and orientations are compared below to the calculated stress field around plane strain and radial pressurized fractures.

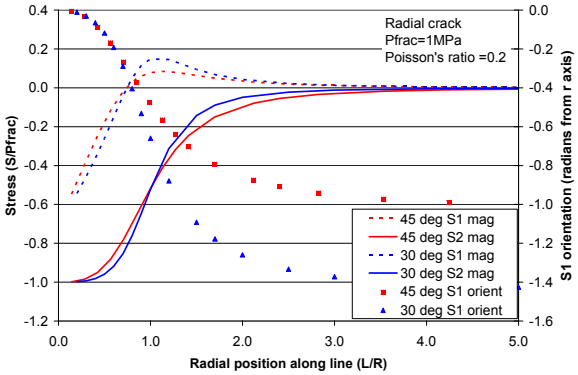

Fig. 5: Calculated stress components and orientation along selected lines near a radial fracture.

4.3. Stress trajectories

The stress change data records the magnitude and orientation of the stress at the location of the instrument. The relative size and position of the fracture with respect to the location of the stress change cell must be known to interpret the data but it is desirable to use the stress change data to infer information about the fracture size and orientation.

An overall view of the stress field orientation around a fracture is provided by a stress trajectory plot. Stress trajectories are lines that satisfy the condition that they are tangent to principal stress directions. In two dimensions, the stress trajectories make up a mesh or net consisting of two sets of lines that intersect always at 90 degrees. Furthermore, the spacing between stress trajectories is reduced as the stress magnitude increases. In this section the stresses around fractures will be represented by stress bar plots rather than stress trajectories.

The stress bar plots are obtained numerically using a finite element model (Wawrzynek and Ingraffea [4]). The model plots the principal stress at integration points in each element using two short lines. The orientation of the line corresponds to the orientation of that principal stress and the length of the line corresponds to the stress magnitude. Spacing between the points, therefore, depends on the finite element mesh rather than on the magnitude of the stress. The stress bar plots presented here have been further divided into two plots for each fracture studied, one plot contains compressive stress bars and the other contains tensile stress bars.

Fig. 6 shows the compressive stress bars around a radial fracture with internal uniform pressure. No

far-field stresses load the fracture so the stress field generating the stress bars shown represents the stress changes that occur as a result of only the pressurised fracture. The corresponding plot for tensile stress bars is contained in Fig. 7.

The stress bar plots show that significant regions of tensile stress exists in front of and near the tips of the fracture and that compressive stresses exist along either side behind the leading edge. The stresses change orientation with position near the leading edge and the compressive stress in the center part of the fracture is aligned to be perpendicular to the fracture plane. It should be emphasized here that, at the site, the far-field compressive stresses were present and were much higher in magnitude than the stress changes from the fracture. The complete stress field was therefore compressive everywhere except very near the tip of the fracture. The stress change cells sense the change in this compressive stress field and the tensile stress as shown in Fig. 7 would be measured as tensile-going stress changes.

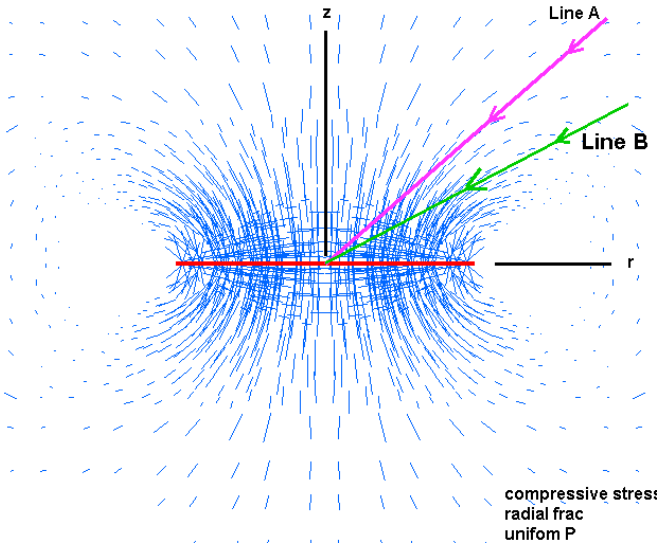

Fig. 6: Opening fracture – compression stress bars.

4.4. Stress change and relative location of cells

The stress change cells are bonded to the rock in boreholes located near the hydraulic fracture plane. Initially the fracture starts some distance from this location as a small fracture growing from a separate injection borehole. As the hydraulic fracture grows in size its leading edge approaches and then passes the location of the stress change cell. The fracture is then extended in size during the rest of the injection and it eventually becomes large compared with the distance between the stress change cell and the hydraulic fracture plane.

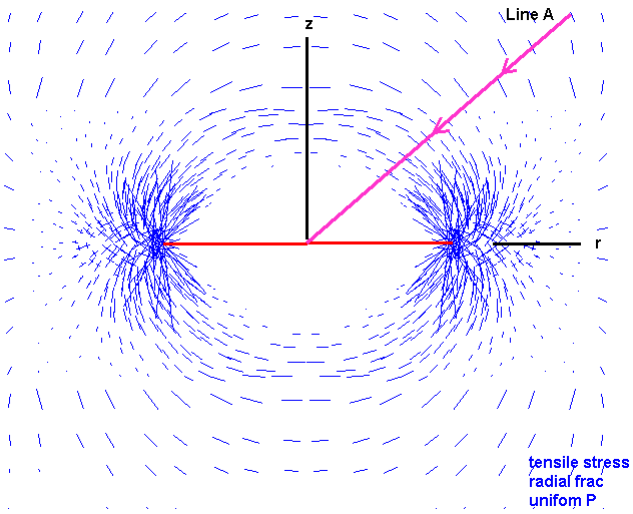

Fig. 7: Opening fracture – tension stress bars.

A single stress bar plot can be used to represent stress at the stress change cell at different times and for different sizes of the hydraulic fracture. For example, if a stress change cell is located along the z-axis of a radial hydraulic fracture, it will never be passed by the leading edge. But as the fracture grows in size the normalized distance from the cell to the fracture center, measured in units of fracture radius (z/R), becomes smaller. Therefore, the stress path felt by the cell can be shown in Figs. 6 or 7 as a straight line along the z-axis, with both axes now rescaled as z/R and r/R. The stress cell moves from an initial position at great z/R on this line (small R) to a position close to the fracture corresponding to later times when the fracture is large (large R).

A similar straight virtual path is followed for a cell located at any point around the fracture. If the fracture grows symmetrically, the position (r/R,z/R) of the point moves from an initially distant location along a straight line toward the center of the fracture. Line A in Figs. 6 and 7 illustrates such a virtual path for a cell located at 45 degrees from the axis of the hydraulic fracture. Alternatively, the stress at each point along such a virtual path can be calculated using the solution for stress around a pressurised fracture (Fig. 5).

Hydraulic fractures typically propagate as opening mode fractures with the fluid pressure acting to open and extend them. In naturally fractured rock, fluid injection can pressurize natural fractures that are oriented at an angle to the principal stress direction. In such cases, the fracture may deform in a shear mode. Fig. 8 shows the stress bar plot for compressive stress around a fracture subject to a far-field shear stress only. The stress change data recorded can be used to determine if dilating shear

fracture growth was a primary fracture mode at the site.

5. STRESS CHANGE AND FRACTURE GROWTH

Stress change cell AN2 was located 10.2 m west, 6.9m north and 15.1 m above the fracture initiation point. For the analysis of fracture growth, it is convenient to take the fracture initiation point as the center of the fracture and as the origin of a fracture coordinate system. Furthermore, the fracture is assumed to be radial in shape and oriented so its plane is vertical and striking north-south. AN2 then lies on a ray from the center of the fracture that is 19.5 m long and at an angle of 31 degrees with the plane of the fracture. If the coordinate system is normalized by the fracture radius, the stress state experienced by the cell as the fracture grows symmetrically is represented in Fig. 6 (for example) by a straight line (Line B). The r/R axis is aligned along the vertical direction and the z/R axis points in to the west.

The stress change can now be calculated for points along line B, corresponding to growth of the fracture. The 30 degree data in Fig. 5 corresponds to such a calculation for the location of AN2 with respect to fracture 2.

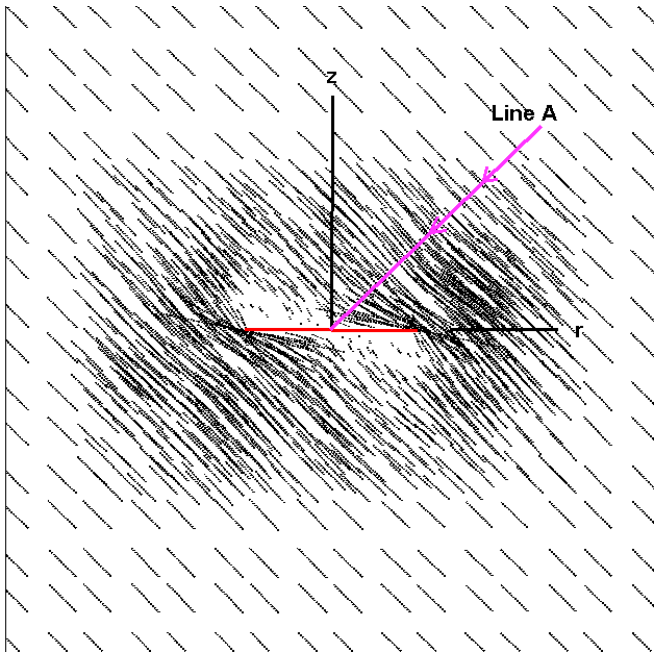

Fig. 8: Shear fracture – compression stress bars.

The stress change given by the 30 degree data in Fig. 5 can be transformed to stress change with time so that it can be compared with the measured stress change. The transformation requires the use of measured fracture growth data obtained from other instruments at the site. The fracture growth rate was measured as it grew through remote pressure monitoring holes located at various distances from the injection hole. From these intersections, a best-fit growth relationship was determined in the form of a power law.

$$R = At^b \qquad (3)$$

where A and b are coefficients determined by fitting the measured data, R is the fracture radius in meters, and t is time in minutes. Eq. 3 can be rewritten to give time as a function of fracture radius, R, as:

$$t = \left(\frac{R}{A}\right)^{1/b} \qquad (4)$$

which then can be used to transform the relative size on the x-axis of Fig. 5 into injection time.

After making this change in the data in Fig. 5, the measured stress change and the modeled stress change can be displayed together in one plot (Fig. 9). The sign of the model stresses have been changed in this plot so that compressive stress is now shown as positive, which agrees with the sign convention for the measured data.

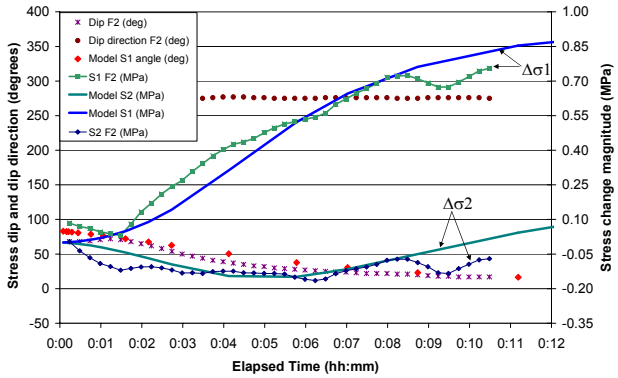

Fig. 9: Modeled and measured stress change for fracture 2 and for cell AN2.

The model fits the measured data very well, both for stress magnitude and for stress direction for the maximum principal stress change. The fit to the measured change in the other principal stress is less good, but the data and model follow the same trend. Other stress change cells for both fractures 1 and 2 produced similar good results. The fit obtained between the data and the model is evidence that the hydraulic fractures were nearly vertical and grew according to the average growth curve obtained from other measurements.

The stress change around a shear fracture would result in different stress magnitudes acting at a nearly constant angle to the fracture plane (Fig. 8). Attempting to fit the measured data with a model

for shear fracture growth would not be possible, which confirms that the hydraulic fractures grew in opening-mode.

Fig. 9 contains plots of stress change components on a vertical plane aligned with the fracture. Tensile going stresses occurred in the data for 2.5 to 3 minutes during the first part of each fracture treatment and, from other measurements at the site, the fracture growth velocity can be calculated using Eq.(3). Based on the measured growth data, the tensile going zone is estimated to be 11 to 14m in size, ahead of the compressive going zone at the time the fracture leading edge passes the instrument. Fig. 9, which shows the measured data and stress change data from a radial model, shows a fairly good fit between the measured and modeled stress components. The relatively large tensile going period is seen, from this figure, to coincide with the effect of the stress component labeled $\Delta\sigma_2$ in that diagram.

A contour plot of $\Delta\sigma_z$ is shown in Fig. 10. From this plot it can be seen that the change from tensile to compressive $\Delta\sigma_z$ (the zero contour) is defined by a line that runs nearly orthogonal to the fracture tip. Therefore, if the fracture orientation is know, a plot of $\Delta\sigma_z$ along the direction of the fracture will locate the fracture leading edge.

This information can then be used to obtain the fracture growth rate from initiation to its passing the instrument, which is useful information to confirm or improve the fracture design. As discussed above, the fracture orientation can be obtained from the orientation of the maximum stress change vectors for times that correspond to a large fracture size relative to the position of the stress change instrument.

6. DISCUSSION

The stress change measurements provide information about important parameters concerning the mechanics of hydraulic fracture growth. The stress change direction and magnitude data can be interpreted in a straight forward way to give information about the fracture orientation. The initial stress change is influenced by the approaching leading edge of the fracture, but once the fracture is large compared with the distance from the instrument to the fracture plane, the maximum stress change vector is oriented nearly orthogonal to the fracture plane, providing an orientation measurement.

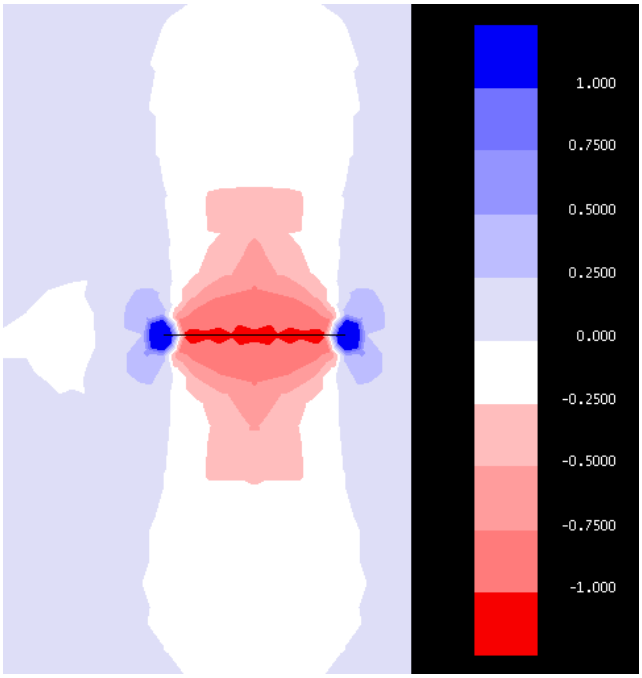

Fig. 10: Contours of $\Delta\sigma_z$ around radial fracture.

The stress change instruments are sensitive enough to detect the small fracture forming at the borehole early in the fracture initiation process. This information, when combined with data from a model giving stress around the fracture, can be used to estimate the fracture growth rate over a distance that is on the same order as the distance from the instrument to the borehole initiation point.

Later stress change data is dominated by the compressive stress around the fracture generated by the excess fluid pressure and the fracture opening. The magnitude of the excess pressure is reflected in the magnitude of the maximum principal stress change component.

Finally, the mode of fracture growth can be determined by comparing the stress change with time, as the hydraulic fracture grows, to the stress field existing around either an opening mode or a shear mode fracture.

7. CONCLUSIONS

The stress change data confirms that the hydraulic fractures grew as opening-mode rather than shear mode fractures. Stress change calculated using a radial fracture geometry model with the fracture opened by a uniform pressure fit the measured stress change quite well. The fit obtained helps establish the orientation and growth rate for the fractures generated at the site.

The stress change data can be used to infer the orientation of the hydraulic fracture, the fracture growth rate, and the excess pressure in the fracture.

REFERENCES

1. Mills, K.W. 1997. In situ stress measurement using the ANZI stress cell. *Proceedings of the International Symposium on Rock Stress,* 149-152. Rotterdam:Balkema.

2. Pollard, D.D. and P. Segall. 1987. Theoretical displacements and stresses near fractures in rock: with application to faults, joints, veins, dikes, and solution surfaces. Chapter 8 in *Fracture Mechanics of Rock*. B.K. Atkinson editor, Academic Press, London.

3. Sneddon, I.N. 1946. The distribution of stress in the neighbourhood of a crack in an elastic solid. *Proceedings Royal Soc. Of London,* 229-260.

4. Wawrzynek, P., and Ingraffea, A. 1995. FRANC2D – A two dimensional crack propagation simulator, *User's Guide*. Version 2.7, Cornell Fracture Group